Desalination and Water Treatment
www.deswater.com
doi: 10.5004/dwt.2023.29878

309 (2023) 193–199
October

Improved performance of vacuum membrane distillation process

Suhaib M. Alawad[a,*], Atia E. Khalifa[a,b]

[a]*Interdisciplinary Research Center for Renewable Energy and Power Systems (IRC-REPS), email: suhaib.ahmed@kfupm.edu.sa (S.M. Alawad)*
[b]*Mechanical Engineering Department, King Fahd University of Petroleum and Minerals, Dhahran, Saudi Arabia*

Received 30 June 2023; Accepted 23 August 2023

ABSTRACT

This study presents a theoretical model based on integrated heat and mass transfer in a vacuum membrane distillation module. The vacuum membrane distillation is being investigated using a parametric analysis with the objective of investigating the influence of operating parameters on process performance. The study considers various factors associated with VMD operation, such as feed inlet temperature, feed inlet flowrate, and vacuum pressure. Two key performance metrics, namely permeate flux and gained output ratio (GOR), are employed to evaluate the system's performance. The results reveal that raising the feed temperature and flowrate results in improved output flux and GOR. Nevertheless, the impact of changing the feed temperature on performance enhancement surpasses that of adjusting the feed flowrate. Furthermore, decreasing the pressure in the permeate channel, thereby achieving higher vacuum levels, significantly improves the permeate flux, particularly at lower feed temperatures. However, this productivity increase comes at the expense of increased heat loss and reduced GOR. Additionally, all the parameters investigated demonstrate substantial effects on the permeate flux, while their influences on the GOR are negligible.

Keywords: Water desalination; Vacuum membrane distillation; Theoretical analysis; Performance and energy evaluation

1. Introduction

Membrane distillation (MD) is a desalination process that uses a hydrophobic membrane to separate freshwater from seawater by means of thermal gradients. The process works by heating the seawater on one side of the membrane; the membrane separates vapor that is then condensed on the other side of the membrane to produce freshwater [1,2]. The membrane is designed to allow the water vapor to pass through while preventing the liquid water and dissolved salts from passing through. The MD process relies on a temperature gradient to create a vapor pressure gradient to drive the water molecules through the membrane. This allows MD to operate at lower pressures, making it more energy-efficient than thermal distillation methods [3]. MD has other pros over the conventional desalination methods, it has a higher tolerance to the presence of dissolved salts and other impurities in the feed water, it can operate at relatively low temperatures, and it is less sensitive to fouling. However, the technology is still considered in early stages of development, and it is not yet widely used in commercial desalination plants [4,5].

There are four primary configurations in membrane distillation (MD) that are classified based on how water vapor condenses while permeating through the membrane: direct contact membrane distillation (DCMD), sweeping gas membrane distillation (SGMD), air gap membrane distillation (AGMD), and vacuum MD (VMD) [6]. Among these designs, VMD demonstrates the greatest system efficiency due to its minimal conduction heat loss and substantial water productivity. In the VMD process, vacuum pressure is utilized to create a difference in water vapor pressure between the hot and cold sides instead of introducing a cold stream to the permeate side. As a result, temperature

* Corresponding author.

Presented at the European Desalination Society Conference on Desalination for the Environment: Clean Water and Energy, Limassol, Cyprus, 22–26 May 2023

1944-3994/1944-3986

polarization and conduction loss are greatly reduced in VMD. Additionally, the application of vacuum on the cold side eliminates air from the membrane pores, leading to negligible molecular diffusion and a uniformly maintained vacuum level on the cold side. Consequently, mass transfer through the membrane pores is predominantly governed by Knudsen diffusion [7].

Several investigators have studied and assessed the performance of the VMD process for different applications. In this regard, Zhang et al. [8] proposed and numerically investigated a novel micro VMD system with semicircular spacers through a computational fluid dynamics approach. Including these semicircular spacers in the VMD, the system brought about modifications in the flow field, reducing mass transfer resistance and improving the system's permeate flux and temperature polarization coefficient. The results demonstrated a uniform temperature distribution when the semicircular spacers were employed.

Another experimental study [9] examined the performance of a novel hollow fiber VMD system with holes in its central tube. By incorporating a perforated central tube, the average vapor pressure was effectively reduced. The study also proposed the optimal parameters for the packing fraction, length, and suction mode of the system. The findings indicated that the utilization of double-suction resulted in a more uniform pressure distribution. This configuration not only reduced the specific energy consumption (SEC) by 12.5% but also improved the flux by 50%–70% compared to the single suction configuration.

In their work, Han et al. [9] introduced a conductive heating VMD system designed for brine desalination. This system implemented conductive heating by attaching an aluminum shim to the membrane, effectively mitigating the adverse impact of temperature polarization on membrane distillation. The results showed promising outcomes, including a maximum water flux of 9.8 $kg/m^2 \cdot h$. Notably, the temperature polarization coefficient surpassed one, leading to an exceptional improvement in the system's thermal efficiency, reaching a maximum value of 83.2%.

Different studies have been carried out to improve the productivity of the VMD process. Most of these studies have been conducted for small-scale systems, and some have used multistage systems for productivity improvement (e.g., [10,11]). The current study aims to enhance the performance of the VMD process through a detailed performance analysis of a large-scale vacuum membrane distillation system and the determination of the best conditions. The performance of the VMD system is evaluated in terms of permeate flux and gained output ratio (GOR). The investigated operating parameters involve the influence of feed temperature, feed flowrate, and vacuum pressure.

2. System description

As depicted in Fig. 1, the feed solution undergoes heating to reach the desired temperature with the assistance of an electric water heater. Subsequently, the heated feed solution is introduced into the VMD module through the feed channels. Within the module, the feed solution flows over the surface of a hydrophobic membrane, with a maintained pressure disparity between the two sides of the membrane. To prevent deflection of the membrane caused by the pressure exerted by the feed stream, a metal sheet equipped with multiple holes supports the membrane. At the liquid-membrane interface, a portion of the feed solution evaporates. The pressure variation across the membrane prompts the resulting vapor to permeate through the membrane while the remaining liquid is directed back to the water heater for heating and recirculation. To enhance the separation of water vapor from the feed solution, a vacuum pump is employed to remove the water vapor once it has traversed the membrane, thereby maintaining a low pressure on the permeate side. The evacuated water vapor is then directed to an external condenser, where it undergoes condensation, leading to the formation of a purified permeate stream. The condenser is maintained at a lower temperature with the aid of cold water supplied by an electric chiller. The membrane used in the module has a thickness of 7 μm and a porosity of 0.8. The diameter of the membrane pores is 0.45 μm. The effective membrane area for the module is 1 m^2. The dimensions of the feed channels within the MD module are 0.5 m in width, 0.7 m in length, and 0.01 m in depth. The module consists of 3 channels in total.

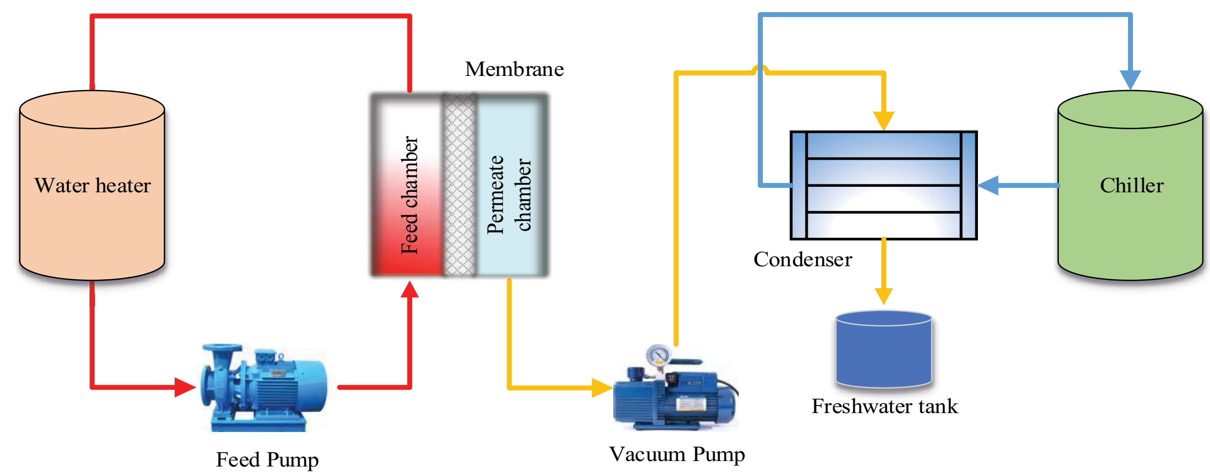

Fig. 1. Schematic diagram of vacuum membrane distillation process.

3. Theoretical approach

In this section, the thermodynamic performance of the proposed VMD system is evaluated via mathematical modeling. A listing of all of the heat and mass transfer equations in both the MD module and the external condenser, as well as the performance indices, are displayed in Table 1. To investigate the performance of the proposed system, two performance indices are used, including the permeate flux and the gained output ratio (GOR).

4. Results and discussion

In this section, the influences of the main operational parameters on the performance of the VMD process are examined. The operating parameters include; the feed inlet temperature, feed inlet flowrate, and vacuum pressure. At the same time, the metrics for evaluating performance include the output flux and the gained output ratio (GOR).

5. Effect of feed temperature

In the MD process, the primary factor driving vapor permeation through the membrane is the variation in vapor pressure created by the temperature variation between the two sides of the membrane. Therefore, it is crucial to examine the influence of the hot water temperature on the overall performance of the system. Fig. 2 illustrates the influence of feed water temperature on the system performance. In this case, the hot water temperature is changed from 50°C to 90°C, whereas other parameters are constant, as mentioned below the figure. As depicted in Fig. 2a, raising the temperature of the feed water leads to an enhancement in the output flux. Specifically, elevating the hot water temperature from 50°C to 90°C results in a substantial improvement in the system's permeate flux, rising from 11.6 to 254 kg/m²·h (approximately a 2,000% enhancement). This increase in permeate flux can be attributed to the larger temperature difference across the membrane, which generates a stronger driving force for vapor generation and permeation, thereby

Table 1
Heat and mass transfer equations

Heat and mass transfer in the MD module		
Rate of energy transfer from feed stream to the membrane [12,13]	$Q_{\text{feed}} = h_f \times \left(T_f - T_{\text{mf}}\right) \times A_f$	(1)
Heat transfer through the membrane by conduction and vapor transfer [14]	$Q_{\text{mem}} = \left(\frac{k_{\text{cm}}}{\delta}\right)\left(T_{\text{mf}} - T_{\text{ms}}\right) \times A_f + J_W \times \Delta H_v \times A_v$	(2)
Heat transfer through the support plate [3,15]	$Q_{\text{sp}} = \left(\frac{k_{\text{sp}}}{\delta_{\text{sp}}}\right)\left(T_{\text{ms}} - T_{\text{sg}}\right) \times A_{\text{sp}} + \left(\frac{k_{\text{cm}}}{\delta}\right)\left(T_{\text{mf}} - T_{\text{ms}}\right) \times A_v + \left(J_w \times \Delta H_v\right) \times A_v$	(3)
Vapor mass flux [16]	$J_w = D_e \times \left(P_{\text{mf}} \times \gamma_{\text{wf}} \times X_{\text{wf}} - P_{\text{mp}}\right)$	(4)
Equivalent diffusion coefficient [17]	$D_e = \left(\frac{\alpha}{D_k} + \frac{1-\alpha}{D_m}\right)^{-1}$	(5)
Knudsen diffusion coefficient [17]	$D_k = \left(\left(\frac{3 \times \delta \times \tau}{2 \times \varepsilon \times d_{\text{pore}}}\right)\left(\frac{\pi \times R \times T_m}{8 \times M_w}\right)^{0.5}\right)^{-1}$	(6)
Molecular diffusion coefficient [17]	$D_m = \left(\frac{R \times T_m \times \delta \times \tau \times P_{\text{air-pore}}}{M_w \times \varepsilon \times PD_{w,a}}\right)^{-1}$	(7)
Heat & mass transfer in the condenser		
Heat transfer inside the condenser [18]	$Q_{\text{condenser}} = U_c \times A_s \times \text{LMTD} = \dot{m}_v \times h_{\text{fg}}$	(8)
Performance indices		
Permeate flux	$\text{Flux} = \left(\frac{\dot{V}_d \times \rho}{A_v}\right)$	(9)
Gained output ratio (GOR)	$\text{GOR} = \left(\frac{J_w \times \Delta H_v \times A_v}{Q_{\text{in}}}\right)$	(10)

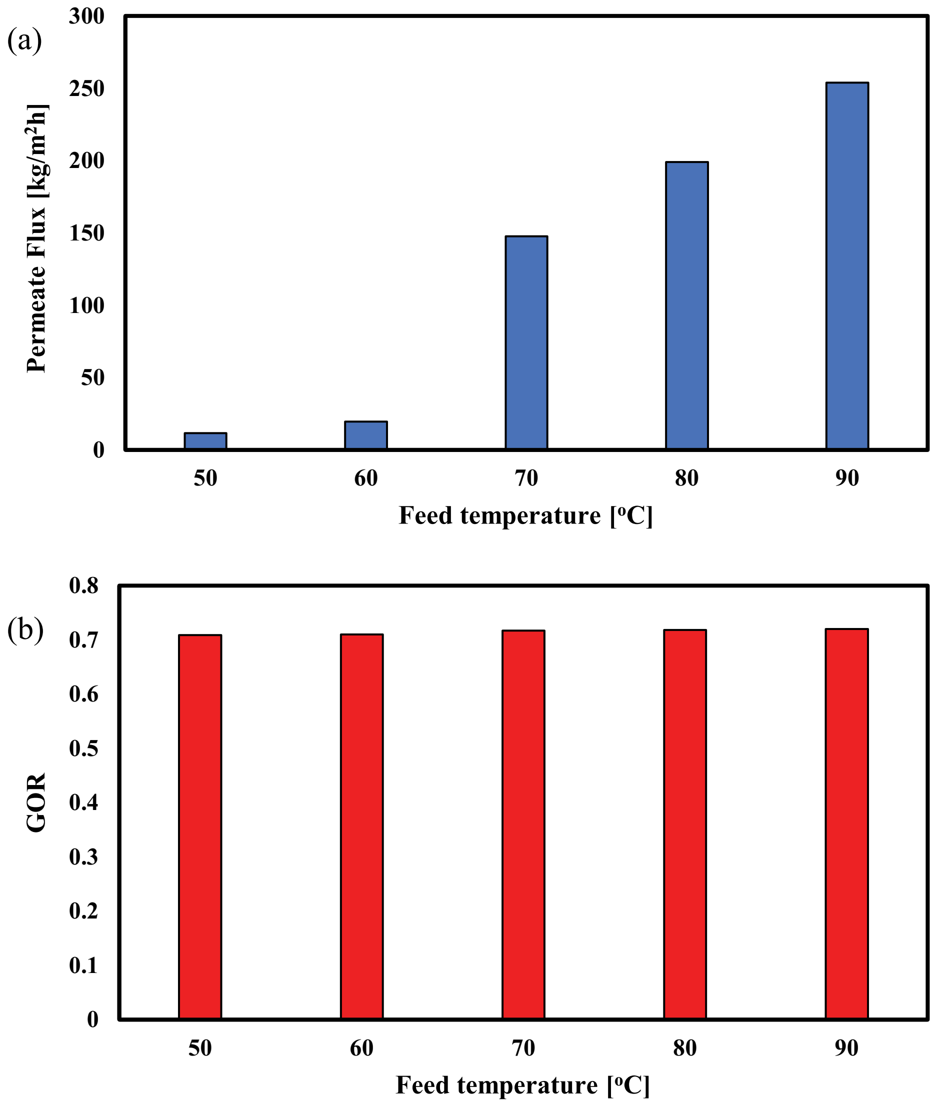

Fig. 2. The variations of permeate flux and GOR with feed temperature. Conditions: cold water temperature of 20°C, feed and coolant flowrates of 50 L/min, condenser area of 3 m^2, and vacuum pressure of 55 mbar.

boosting the system's productivity. In Fig. 2b the variation of the system's gained output ratio (GOR) with feed water temperature is demonstrated. It is observed that the system's GOR improves as the feed water temperature rises from 50°C to 90°C, with a peak GOR value of 0.72 and an overall increase of approximately 2%. This improvement in GOR is primarily driven by the exponential growth in system flux as the hot water temperature increases. Although energy consumption also increases with higher feed water temperature, it is noteworthy that the system's recovery ratio demonstrates improvement with the elevated feed water temperature. This is due to the higher permeation of vapor across the membrane pores at higher feed water temperatures.

6. Effect of feed flowrate

The impact of the feed water flowrate on the output flux is depicted in Fig. 3a. It is evident that raising the flowrate of the feed stream results in an improvement in the output flux. This enhancement can be attributed to the higher turbulence level of the flow and the consequent reduction in the thermal boundary layer thickness on the membrane hot side. These changes facilitate higher coefficients of mass and heat transfer on the feed side of the membrane, resulting in an overall enhancement in system productivity. It is important to note that at a feed flowrate of 10 and 30 L/min, the flow is characterized as laminar, while it transitions to a turbulent flow at a flowrate of 50 L/min. This transition from laminar to turbulent flow is the reason for the relatively greater growth in output flux when the flowrate changes from 10 to 50 L/min. However, increasing the flowrate beyond 50 L/min leads to a comparatively smaller improvement in output flux. For instance, when the feed water flowrate changes from 10 to 50 L/min, the output flux improves by over 800%. In contrast, when the flowrate is further raised from 50 to 90 L/min, the permeate flux shows an improvement of about 37%.

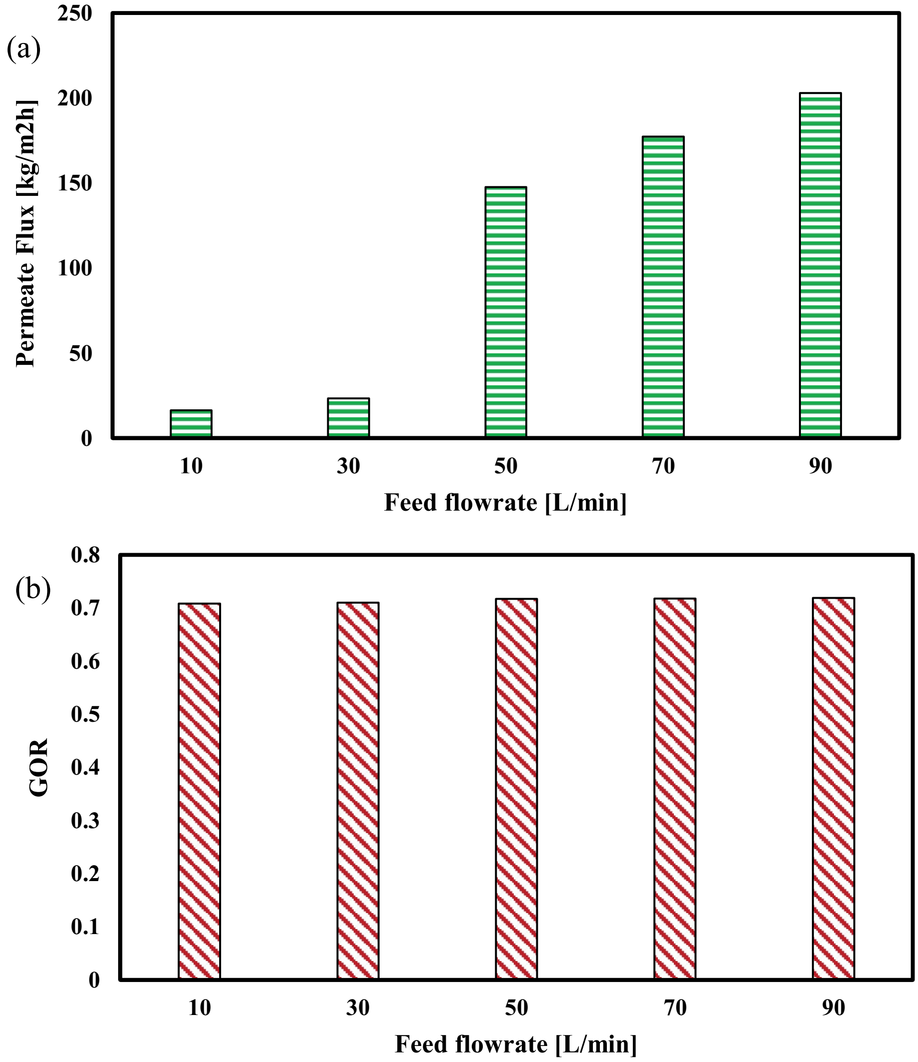

Fig. 3. The variations of permeate flux and GOR with feed flowrate. Conditions: cold water temperature of 20°C, coolant flowrate of 50 L/min, feed temperature of 70°C, condenser area of 3 m^2, and vacuum pressure of 55 mbar.

Fig. 3b presents the influence of the hot water flowrate on the system's gained output ratio (GOR). The figure demonstrates that the system's GOR improves as the feed water flowrate increases. Specifically, increasing the feed flowrate from 10 to 90 L/min results in a slight enhancement of approximately 1.5% in the system's GOR. This improvement in GOR at higher feed flowrates can be attributed to the overall improvement in system productivity. While a higher feed flowrate requires more energy, in this scenario, the influence of increased energy consumption is overshadowed by the higher productivity achieved at the elevated feed flowrate. As a result, the recorded improvement in GOR at the high feed water flowrate can be attributed to the enhanced productivity outweighing the impact of increased energy consumption.

7. Effect of vacuum pressure

The vacuum pressure is another crucial operational parameter in the VMD process, as the permeation rate is directly influenced by the vapor pressure variance across the membrane. Fig. 4a illustrates the variations of the permeate flux with the vacuum pressure. In general, reducing the vacuum pressure leads to a substantial improvement in the output flux. However, it is observed that reducing the vacuum pressure has a more pronounced effect at lower feed temperatures. For instance, when the vacuum pressure in the permeate channel is reduced from 85 to 5 mbar, there is a remarkable (around 490%) improvement in output flux at a low hot water temperature of 50°C. Nonetheless, this improvement diminishes as the feed temperature rises, reaching approximately 35% at a hot water temperature of 90°C.

The variation of the gained output ratio (GOR) with vacuum pressure is shown in Fig. 4b. It is found that although reducing the vacuum pressure significantly improves productivity in the VMD process, it also leads to increased heat loss on the feed side. This heat loss causes a significant temperature decrease in the feed stream, requiring more energy to heat it back to the desired temperature. For example,

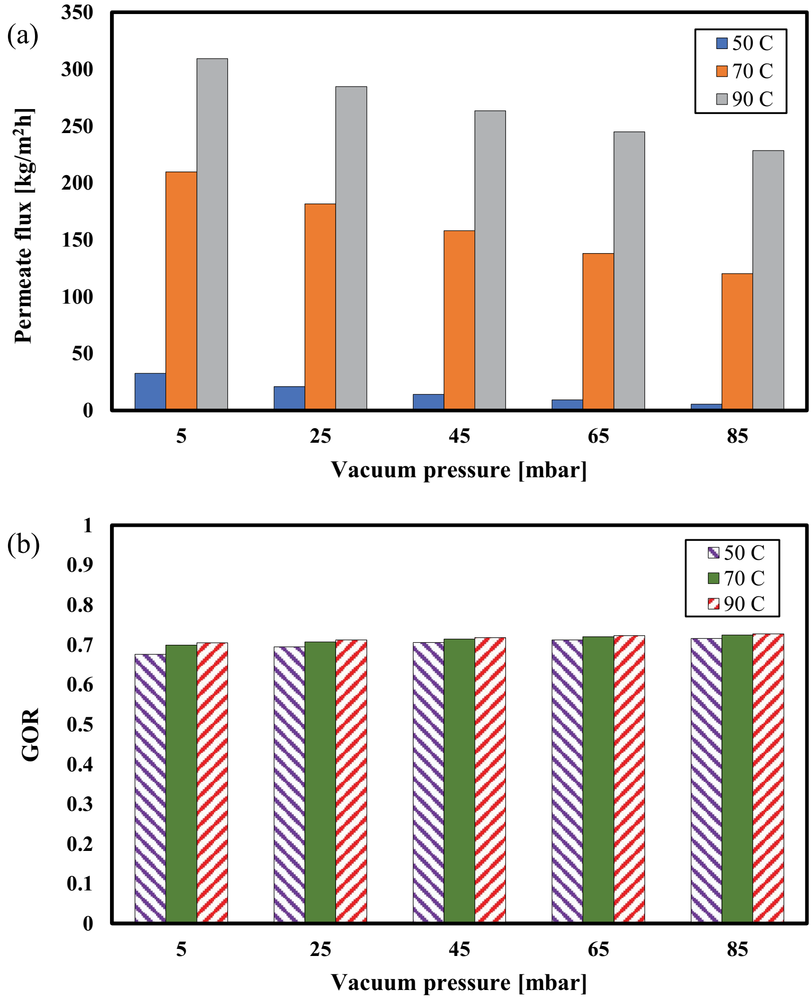

Fig. 4. The variations of permeate flux and GOR with vacuum pressure. Conditions: cold water temperature of 20°C, feed & coolant flowrates of 50 L/min, and condenser area of 3 m^2.

when the hot water inlet temperature is 70°C, and the vacuum pressure is reduced to 5 mbar, the temperature drop in the feed stream is nearly doubled compared to the temperature drop at the same feed inlet temperature but with a vacuum pressure of 85 mbar. Consequently, only a negligible (about 3.5%) reduction in the gained output ratio (GOR) is observed when applying lower pressure in the permeate side of the membrane.

8. Conclusions

This study focuses on the examination of the vacuum membrane distillation (VMD) process through a parametric analysis, aiming to investigate how operating parameters influence the process performance. Various factors related to the operation of the VMD process are investigated, including the feed inlet temperature, feed inlet flowrate, and vacuum pressure. The system performance is evaluated based on two metrics: the output flux and GOR. The results demonstrate that both the output flux and GOR exhibit an increase with higher feed temperature and flowrate. However, the effect of changing the hot water temperature on the performance enhancement is more significant compared to that achieved by adjusting the feed flowrate. Additionally, reducing the pressure in the permeate channel (achieving higher vacuum levels) leads to a notable improvement in the output flux, particularly at lower feed temperatures. It is worth noting, however, that this increase in productivity comes at the cost of increased heat loss and reduced GOR. Furthermore, all the studied parameters have significant impacts on the permeate flux; however, their effects on the GOR are negligible.

Symbols

Q_{feed}	—	Transfer rate of energy in the hot side, W
h_f	—	Coefficient of heat transfer in hot water channels, W/m^2·K
T_f	—	Temperature of the bulk feed, °C
T_{mf}	—	Hot water temperature at the membrane surface, °C
A_f	—	Heat transfer area in the feed side, m^2
Q_{mem}	—	Transfer rate of energy across the membrane, W

k_{cm} — Membrane conductivity, W/m·K
δ — Thickness of membrane, m
T_{ms} — Temperature of the membrane at the support plate surface, °C
J_w — Mass flux of water vapor, kg·m²·s
ΔH — Enthalpy of evaporation, J/kg·K
A_v — Effective area of membrane, m²
Q_{sp} — Transfer rate of energy across the support plate, W
k_{sp} — Supporting plate conductivity, W/m·K
δ_{sp} — Thickness of supporting plate, m
T_{sg} — Temperature of the support plate at the gap side, °C
A_{sp} — Heat transfer area in the support plate, m²
D_e — Diffusion coefficient, m²/s
P_{mf} — Vapor pressure in the hot surface, Pa
P_{mp} — Vapor pressure in the cold surface, Pa
γ_{wf} — Activity factor, –
X_{wf} — Salinity of the feed water, g/L
α — Ratio of Knudsen to mass diffusions, –
D_k — Knudsen diffusion coefficient, m²/s
D_m — Mass diffusion coefficient, m²/s
τ — Membrane tortuosity, –
ε — Membrane porosity, –
d_{pore} — Pore diameter, m
R — Gas constant
T_m — Mean temperature of membrane, K
M_w — Molecular mass of water, kg/Kmol
$P_{airpore}$ — Pressure of the air within the membrane
$Q_{condenser}$ — Rate of energy transfer in the condenser, W
U_c — Overall heat transfer coefficient, W/m²·K
A_s — Heat transfer area in the condenser, m²
$\dot{m}_v$ — Vapor mass transfer, kg/s
h_{fg} — Enthalpy of evaporation of the water vapor, J/kg·K
$\dot{V}_d$ — Volume flow rate of the distillate, m³/h
ρ — Water density, kg/m³
Q_{in} — Energy used for heating and cooling, W

Acknowledgement

The authors acknowledge the financial support received from IRC for Renewable Energy and Power Systems, KFUPM, under Research Grant no. INRE2206.

References

[1] S.M. Alawad, A.E. Khalifa, Development of an efficient compact multistage membrane distillation module for water desalination, Case Stud. Therm. Eng., 25 (2021) 100979, doi: 10.1016/j.csite.2021.100979.
[2] S.M. Alawad, A.E. Khalifa, M.A. Antar, M.A. Abido, Experimental evaluation of a new compact design multistage water-gap membrane distillation desalination system, Arabian J. Sci. Eng., 46 (2021) 12193–12205.
[3] S.M. Alawad, A.E. Khalifa, Analysis of water gap membrane distillation process for water desalination, Desalination, 470 (2019) 114088, doi: 10.1016/j.desal.2019.114088.
[4] A. Alkhudhiri, N. Darwish, N. Hilal, Membrane distillation: a comprehensive review, Desalination, 287 (2014) 2–18.
[5] Y.-D. Kim, K. Thu, N. Ghaffour, K. Choon Ng, Performance investigation of a solar-assisted direct contact membrane distillation system, J. Membr. Sci., 427 (2013) 345–364.
[6] K.W. Lawson, D.R. Lloyd, Membrane distillation. I. Module design and performance evaluation using vacuum membrane distillation, J. Membr. Sci., 120 (1996) 111–121.
[7] J.G. Lee, W.S. Kim, Numerical study on multi-stage vacuum membrane distillation with economic evaluation, Desalination, 339 (2014) 54–67.
[8] Z. Zhang, N. Zhang, B. Xiang, Y. Yuan, P.E. Phelan, Numerical investigation on mass and heat transfer performance for novel vacuum membrane distillation modules enhanced by semicircular spacers, Int. J. Therm. Sci., 187 (2023) 108165, doi: 10.1016/j.ijthermalsci.2023.108165.
[9] F. Han, Y. Bian, C. Zhang, Conductive heating vacuum membrane distillation for brine desalination: study on operational conditions, temperature polarization and energy consumption, Desalination, 531 (2022) 115726, doi: 10.1016/j.desal.2022.115726.
[10] P. Sharan, T.J. Yoon, H. Thakkar, R.P. Currier, R. Singh, A.T. Findikoglu, Optimal design of multi-stage vacuum membrane distillation and integration with supercritical water desalination for improved zero liquid discharge desalination, J. Cleaner Prod., 361 (2022) 132189, doi: 10.1016/j.jclepro.2022.132189.
[11] Y. Zhang, Y. Peng, S. Ji, J. Qi, S. Wang, Numerical modeling and economic evaluation of two multi-effect vacuum membrane distillation (ME-VMD) processes, Desalination, 419 (2017) 39–48.
[12] S. Srisurichan, R. Jiraratananon, A.G. Fane, Mass transfer mechanisms and transport resistances in direct contact membrane distillation process, J. Membr. Sci., 277 (2006) 186–194.
[13] T.-C. Chen, C.-D. Ho, H.-M. Yeh, Theoretical modeling and experimental analysis of direct contact membrane distillation, J. Membr. Sci., 330 (2009) 279–287.
[14] C.-K. Chiam, R. Sarbatly, Membranes and theoretical modelling of liquid-gas membrane separation for aromatic compounds removal from water: a review, Int. J. Global Environ. Issues, 12 (2012) 130–149.
[15] S.M. Alawad, A.E. Khalifa, M.A. Antar, Performance analysis of multistage water gap membrane distillation system with economic evaluation, Appl. Therm. Eng., 184 (2020) 116297, doi: 10.1016/j.applthermaleng.2020.116297.
[16] K.W. Lawson, D.R. Lloyd, Membrane distillation, J. Membr. Sci., 124 (1997) 1–25.
[17] S.M. Alawad, D.U. Lawal, A.E. Khalifa, I.H. Aljundi, M.A. Antar, T.N. Baroud, Analysis of water gap membrane distillation process with an internal gap circulation propeller, Desalination, 551 (2023) 116379, doi: 10.1016/j.desal.2023.116379.
[18] H.T. El-Dessouky, H.M. Ettouney, Fundamentals of Salt Water Desalination, 2002.